Proceedings of ASME Turbo Expo 2011
GT2011
June 6-10, 2011, Vancouver, British Columbia, Canada

GT2011-46342

COMPARATIVE VALIDATION STUDY ON IDENTIFICATION OF PREMIXED FLAME TRANSFER FUNCTION

Luis Tay-Wo-Chong*, Sebastian Bomberg, Ahtsham Ulhaq, Thomas Komarek, Wolfgang Polifke
Lehrstuhl für Thermodynamik
TU München
D-85748, Garching, Germany
Email: tay@td.mw.tum.de

ABSTRACT

The flame transfer function (FTF) of a premixed swirl burner was identified from time series generated with CFD simulation of compressible, turbulent, reacting flow at non-adiabatic conditions. Results were validated against experimental data. For large eddy simulation (LES), the Dynamically Thickened Flame combustion model with one step kinetics was used. For unsteady simulation in a Reynolds-averaged Navier-Stokes framework (URANS), the Turbulent Flame Closure model was employed. The FTF identified from LES shows quantitative agreement with experiment for amplitude and phase, especially for frequencies below 200 Hz. At higher frequencies, the gain of the FTF is underpredicted. URANS results show good qualitative agreement, capturing the main features of the flame response. However, the maximum amplitude and the phase lag of the FTF are underpredicted. Using a low-order network model of the test rig, the impact of the discrepancies in predicted FTFs on frequencies and growth rates of the lowest order eigenmodes were assessed. Small differences in predicted FTFs were found to have a significant impact on stability limits. Stability behavior in agreement with experimental data was achieved only with the LES-based flame transfer function.

NOMENCLATURE

a	Speed of sound
A	Amplitude
CFD	Computational Fluid Dynamics
c	Progress variable
$\mathbf{c}$	Cross-correlation vector
CI	Cycle increment
DTFM	Dynamically Thickened Flame Model
FTF	Flame Transfer Function
F	Thickening factor
f	Downstream Riemann Invariant
g	Upstream Riemann Invariant
$\mathbf{h}$	Unit impulse response vector
L	Length of the UIR
l	Length
LES	Large Eddy Simulation
Ma	Mach number
N	Number of elements
$\dot{Q}$	Heat release rate
R	Reflection coefficient
SI	System Identification
TFC	Turbulent Flame Closure
T	Temperature
$\mathbf{T}$	Transfer matrix
u	Axial velocity
UIR	Unit Impulse Response
URANS	Unsteady Reynolds-Averaged Navier-Stokes
Γ	Auto-correlation matrix
ω	Angular Frequency
ρ	Density
γ	Ratio of specific heats
θ	Phase
σ	Standard Deviation

*Address all correspondence to this author.

Copyright © 2011 by ASME

Superscripts

$\bar{}$	Mean
$'$	Fluctuation

Subscripts

u	At upstream/input port
un	Unburnt
d	At downstream/output port
f	Flame
r	Reference position
t	Turbulent

INTRODUCTION

Stringent emission regulations (for NOx, CO, etc.) have been established for gas turbines. In order to comply with these regulations, lean premixed combustion technology has been introduced for stationary engines. However, this mode of operation makes the combustor prone to blow-out or flashback and in particular to thermoacoustic instabilities [1]. Thermoacoustic instabilities, i.e. a self-excited coupling between fluctuations of pressure, velocity and heat release, can lead to very high levels of pressure pulsations in a combustor, possibly resulting in structural damage [2].

To prevent the appearance of combustion instabilities, it is desirable to carry out a stability analysis of the combustion system early in the design process. Low-order "network models" [3–6] may be used for this task. To perform such analysis, it is necessary to know how the flame responds to flow perturbations. This information may be provided by the flame transfer function (FTF).

Flame transfer functions may be obtained experimentally, using velocity or pressure sensors in combination with chemiluminescence as an indicator of heat release in the flame (see e.g. [7–9] for recent applications). Unfortunately, the experimental determination of FTFs for configurations of technical interest is very difficult and costly. (Semi-)analytical models for the FTF have been also proposed, see e.g. [3, 9–11]. However, it is in general not possible to predict flame responses from first principles. Alternatively, it is possible to determine the FTF with computational fluid dynamics (CFD): First an unsteady CFD simulation is performed to generate time series of fluctuating velocity and heat release rate. Then the FTF is reconstructed from the data using methods from system identification (SI) [11–15].

Reynolds-Averaged Navier-Stokes simulation (RANS, or URANS for "unsteady" or transient cases) remains the main turbulence modeling approach in practical applications due to its comparatively low computational cost. However, its application to complex reacting flows is limited by inadequate turbulence and combustion models. Large Eddy Simulation (LES), on the other hand, is now established as a powerful, albeit computationally expensive, tool for the study of turbulent (reacting) flows. Recent applications of LES have shown its potential for laboratory and industry scale configurations [4, 13, 15, 16]. LES makes possible a more accurate description of the turbulence-flame interaction, as the large turbulent scales are resolved.

Tay et al. [13] have determined the FTF of a perfectly premixed axial swirl burner with LES/SI. The numerical results were validated successfully against experiment, and interpreted in terms of a two time lag model. It was shown that the observed excess in gain of the FTF (amplitudes > 1) can be related to a superposition of acoustic and swirl number fluctuations [7, 9, 11, 17]. The present study continues this work: First, FTFs identified from LES and URANS time series data, respectively, are compared against experiment. Then, a stability analysis using a network model is carried out to assess quantitatively the impact of the discrepancies in the predicted FTFs on eigenfrequencies and growth rates of eigenmodes.

BACKGROUND

Flame Transfer Function

The dynamic response of a flame to a flow perturbation can be represented in the frequency domain by its flame transfer function FTF(ω) (also "frequency response"). It relates fluctuations of mass flow rate or velocity u'_r at a reference position r upstream of the flame to fluctuations of the flame heat release $\dot{Q}'$:

$$\mathrm{FTF}(\omega) = \frac{\dot{Q}'(\omega)/\bar{\dot{Q}}}{u'_r(\omega)/\bar{u}_r} \tag{1}$$

Here fluctuations $\dot{Q}'$ and u'_r are normalized with the respective mean values of heat release $\bar{\dot{Q}}$ and velocity $\bar{u}_r$.

System Identification

In experiment, the velocity u'_r may be measured with Constant Temperature Anemometry or by the multi-microphone method, while the heat release $\dot{Q}'$ of the flame is deduced from chemiluminescence intensity measured with a photomultiplier. Applying harmonic excitation with a loudspeaker or siren at the inlet, the flame transfer function FTF(ω) is computed from time series of fluctuations u'_r and $\dot{Q}'$ with spectral analysis. In the presence of turbulent noise, fairly long time series over several hundred cycles are usually required to achieve good accuracy. If the flame transfer function is required over a range of frequencies, the procedure must be repeated many times, which is tedious and time consuming.

The experimental approach of repeated, single-frequency spectral analysis could in principle also be used to determine the FTF from CFD time series data. However, this would be extremely compute intensive. Instead, advanced methods based on

Copyright © 2011 by ASME

System Identification (SI) have been developed [11–14]. In this framework, the linear dynamics of the flame is represented in the time domain by its Unit Impulse Response (UIR). The FTF is then obtained from the UIR by a z-transform (the discrete time equivalent of the Fourier transform):

$$\mathrm{FTF}(\omega) = \sum_{k=0}^{L} h_k e^{-i\omega k\Delta t} = A(\omega)\, e^{i\theta(\omega)} \tag{2}$$

Here $h_k (k = 0, \ldots, L)$ is the k-th coefficient of the UIR $\mathbf{h}$, with time increment Δt. For sufficiently small levels of perturbation, the response may be assumed to be linear (and time-invariant).

For identification of the FTF, a CFD simulation (URANS or LES) of the system under consideration is set up. Once a statistically steady solution is obtained, the CFD model is excited with a broadband perturbation superimposed on the mean flow. At reference position "r" upstream of the flame, (area-averaged) instantaneous values of axial velocity are exported at each time increment (a multiple of the CFD time step size). The global heat release $\dot{Q}$ is obtained by a volume integration of the heat release over the computational domain and also exported for subsequent post-processing.

In URANS, acoustic fluctuations u'_r and the corresponding flame response $\dot{Q}'$ can be retrieved by simply subtracting the mean values of flow variables from the "instantaneous" values. However, in LES it is not straightforward to differentiate between acoustic and resolved turbulent fluctuations. In order to extract acoustic signals from LES time series data, a characteristics based filter (CBF) has been developed by Kopitz et al. [18], which was used also in this work. The auto-correlation matrix Γ and the cross-correlation vector $\mathbf{c}$ of the time series data $(u'_k, \dot{Q}'_k), k = 0, \ldots, N$ are then calculated as follows:

$$\Gamma_{ij} \approx \frac{1}{N-L+1} \sum_{k=L}^{N} \frac{u'_{k-i}}{\bar{u}} \frac{u'_{k-j}}{\bar{u}} \quad \text{for } i, j = 0, \ldots, L \tag{3}$$

$$c_i \approx \frac{1}{N-L+1} \sum_{k=L}^{N} \frac{u'_{k-i}}{\bar{u}} \frac{\dot{Q}'_k}{\bar{\dot{Q}}} \quad \text{for } i = 0, \ldots, L \tag{4}$$

Here u'_k stands for $u'(t = k\Delta t)$, the subscript "r" has been dropped for ease of notation. Then, the Wiener-Hopf equation, an optimal linear least square estimator, defined by

$$\Gamma \mathbf{h} = \mathbf{c} \tag{5}$$

is inverted to obtain the unit impulse response $\mathbf{h}$ of the flame. A flow chart of the CFD/SI method is given in Fig. 1. Note that although the "unit impulse response" is determined with CFD/SI, the excitation signal applied to the CFD model is not an impulse, but a broadband signal. In this way, turbulent signal contributions are suppressed, and it is possible to obtain the frequency flame response over a range of frequencies from one single CFD run. A review of "Dos and Don'ts" for an optimal identification process is presented in [14].

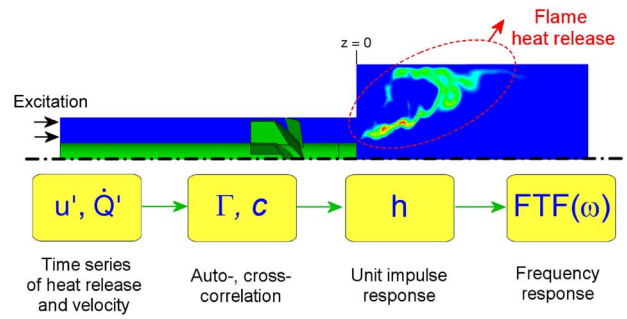

Figure 1. CFD/SYSTEM IDENTIFICATION FLOW CHART.

Low-order Network Models

Low-order network models allow to quickly analyze a (thermo-)acoustic system. The analysis is based on the assumption of linear and time-harmonic acoustics, and is carried out in the frequency domain. The system is represented by a network of acoustic elements. The acoustic variables u', p' – or rather the acoustic waves described in terms of Riemann Invariants f and g [5] – at the upstream/input (u) and downstream/output ports (d) of each element are related by the frequency dependent element transfer matrix $\mathbf{T}$:

$$\begin{pmatrix} f_d \\ g_d \end{pmatrix} = \mathbf{T}(\omega) \begin{pmatrix} f_u \\ g_u \end{pmatrix} \tag{6}$$

The output from one element is passed to the input ports of the next one. Boundary conditions are applied to terminate the system. The assembly of the individual transfer matrices yields a system of equations of the form:

$$\begin{pmatrix} \text{Matrix} \\ \text{of} \\ \text{coefficients } \mathbf{S} \end{pmatrix} \begin{pmatrix} f_m \\ g_m \\ \vdots \\ g_n \end{pmatrix} = \begin{pmatrix} 0 \\ 0 \\ \vdots \\ 0 \end{pmatrix} \tag{7}$$

The characteristic equation $\mathrm{Det}(\mathbf{S}) = 0$ is fulfilled for complex eigenfrequencies, $\omega = \omega_{real} + i\omega_{imag} \in \mathbb{C}$. With harmonic time dependence $\exp(i\omega t)$, the imaginary part of an eigenfrequency indicates whether the corresponding eigenmode grows or decays over time. The cycle increment (CI) of a mode, i.e. the relative growth in amplitude per period of the oscillation, may be defined as [5, 19]:

$$\mathrm{CI} = e^{-2\pi \frac{\omega_{imag}}{\omega_{real}}} - 1 \tag{8}$$

With this definition, $\mathrm{CI} = 0$ corresponds to marginal stability. The real part of the eigenfrequency determines the frequency of the eigenmode.

In the case of a thermoacoustic problem, the flame must be incorporated into the system model. The flame is commonly

Copyright © 2011 by ASME

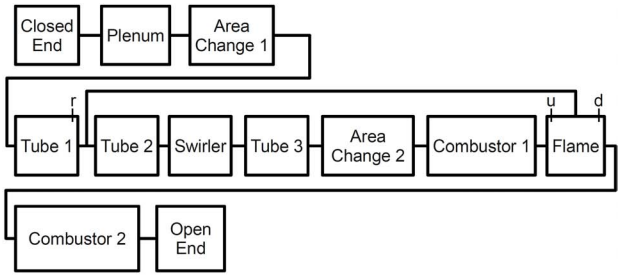

Figure 2. LOW-ORDER MODEL OF PREMIX BURNER TEST RIG.

represented by an acoustically "compact" element. That is, its spatial dimensions are assumed small compared to the acoustic wave length. The acoustic variables at the unburnt (u) and burnt (d) sides of the heat source then satisfy the linearized Rankine-Hugoniot relations [5, 19]:

$$\left(\frac{p'}{\rho a}\right)_d = \frac{(\rho a)_u}{(\rho a)_d}\left[\left(\frac{p'}{\rho a}\right)_u - \left(\frac{T_d}{T_u}-1\right)u'_u \mathrm{Ma}_u\left(1+\frac{\dot{Q}'/\bar{\dot{Q}}}{u'_u/\bar{u}_u}\right)\right] \quad (9)$$

$$u'_d = u'_u\left[1+\left(\frac{T_d}{T_u}-1\right)\frac{\dot{Q}'/\bar{\dot{Q}}}{u'_u/\bar{u}_u}\right] - \left(\frac{p'}{\rho a}\right)_u \mathrm{Ma}_u \gamma\left(\frac{T_d}{T_u}-1\right) \quad (10)$$

In order to obtain a closed system of equations, the heat release fluctuations $\dot{Q}'$ in (9), (10) must be related to the fluctuations in the acoustic variables u' and p'. This is achieved by introducing the FTF from Eq. (1) into Eqs. (9) and (10). In general, the reference location "r", where the input signal u'_r is recorded, is not immediately upstream of the flame at location "u". Thus, the flame is represented as a 6-port element in the network, linking f's and g's at positions "u", "d" and "r", see Fig. 2.

The eigenfrequency analysis requires to evaluate coefficients of the system matrix $\mathbf{S}(\omega)$ also for frequencies $\omega \in \mathbb{C}$ away from the real axis. This requirement is obviously not a problem if analytical expressions for network elements are known [5]. Also, it is not a problem for a flame transfer function determined with CFD/SI, because the argument ω in the z-transform (2) may be complex-valued, such that from the UIR $\mathbf{h}$ the transfer function $\mathrm{FTF}(\omega)$ may be evaluated anywhere in the complex plane.

However, in experiment the flame transfer function is determined with harmonic forcing at constant amplitude, i.e. the FTF is known only for a number of purely real frequencies $\omega_n \in \mathbb{R}$. In such a situation the FTF at intermediate frequencies is often determined by interpolation between measured values. However, for stability analysis the FTF is needed for frequencies away from the real axis. In our experience, extrapolating the FTF from known values on the real axis into the complex plane leads to severe errors: growth or decay of oscillation amplitudes are not properly reflected in the system matrix coefficients, if the imaginary part of the frequency is not taken into account.

To overcome this difficulty with elements that are defined only for purely real frequencies, it is proposed to first compute the UIR by inverse z-transform, and then get corresponding coefficient values for $\omega \in \mathbb{C}$ from forward z-transform. For example, the UIR of an experimental $\mathrm{FTF}(\omega_{real})$ would be obtained as:

$$h_k = \frac{\Delta t}{\pi}\sum_{0}^{\pi/\Delta t}\mathrm{FTF}(\omega_{real})\, e^{i\omega_{real}k\Delta t}, \text{ for } k = 0,\ldots L \quad (11)$$

Turbulent Combustion Modelling

To reduce the complexity of the simulation and the computational requirements, a classical technique is to apply an averaging or filtering procedure to the balance equations. In RANS, the instantaneous balance equations are Reynolds- or Favre-averaged to describe the evolution of the mean quantities. The effect of turbulent fluctuations in the Reynolds stress term, averaged reaction rate, etc. must be modeled to close the system. In LES, the large turbulent scales are calculated explicitly, whereas the effects of smaller ones are modeled using subgrid closures. To separate the large from the small scales, LES is based on a filtering operation considering a filter width. The filter function determines the size and structure of the small scales [4]. Both averaged or filtered equations for reacting flows require the modelling of the reaction source term. In the following, the turbulent combustion models used in this study are presented.

Dynamically Thickened Flame Model for LES

In LES of turbulent flows, the thickness of a premixed flame is typically smaller than the mesh size. Due to this, the reaction source term of the species transport equations needs to be modeled. The idea of the Thickened Flame model, which is based on an Arrhenius formulation, is to increase the flame thickness by a factor F (called "thickening factor") preserving the same laminar flame speed as the unthickened flame, allowing to resolve the flame front on a LES mesh [4, 20]. The Thickened Flame Model applies the thickening in the complete domain. With this, the diffusion in non-reactive zones will be overestimated by a factor F. Legier et al. [21] proposed the Dynamically Thickened Flame Model (DTFM) based on the Thickened Flame Model to overcome this deficiency. In the DTFM, the thickening factor F is not constant, but approaches a maximum value (F_{max}) inside the reaction zone and unity in non-reactive zones. A "sensor" of the reactive zone is used to indicate if the thickening should be applied or not.

Turbulent Flame Closure Model for RANS

In the Turbulent Flame Closure (TFC) combustion model proposed by Zimont and Lipatnikov [22], the flame front propagation is modeled by solving a transport equation for the density-weighted mean reaction progress variable $\tilde{c}$:

$$\frac{\partial(\rho\tilde{c})}{\partial t} + \frac{\partial(\rho\tilde{u}_i\tilde{c})}{\partial x_i} = \frac{\partial}{\partial x_i}\left[\rho D_i \frac{\partial\tilde{c}}{\partial x_i}\right] + \bar{\dot{\omega}} \quad (12)$$

Copyright © 2011 by ASME

The reaction rate source term $\bar{\dot{\omega}}$ and the turbulent burning velocity U_t are modeled as

$$\bar{\dot{\omega}} = \rho_{un} U_t \left|\nabla \tilde{c}\right|, \tag{13}$$

$$U_t = A_{\mathrm{TFC}} G u''^{\frac{3}{4}} S_L^{0\,\frac{1}{2}} \chi_{un}^{\frac{-1}{4}} l_t^{\frac{1}{4}} \tag{14}$$

where ρ_{un}, $\nabla\tilde{c}$, G, A_{TFC}, χ_{un}, S_L^0, u'' and l_t are the density of the unburnt mixture, the gradient of the progress variable, the stretch factor, the model constant equal to 0.52, the thermal diffusivity on the unburnt side of the flame, the unstrained laminar flame speed, the turbulent fluctuation and the turbulent length scale, respectively. A critical strain rate of 8000 s^{-1} was used for calculating the stretch factor.

EXPERIMENTAL SET-UP

A swirl-stabilized "perfectly premixed" burner with an axial swirl generator mounted on a central bluff body was used in this study, see Fig. 3. The burner exit has an annular section with an inner and outer diameter of 16 and 40mm, respectively. The methane-air mixture enters a plenum followed by the burner with an axial swirl generator of 30 mm length. The position of the swirler is 30 mm upstream of the burner exit. The combustion chamber has a quadratic cross section of 90×90 mm. For FTF and OH chemiluminescence measurements, a combustor length of 300mm was used, as it presented stable conditions for different equivalence ratios and power ratings. With a combustor length of 700mm, an instability developed. For the stability analysis, this length was used in combination with a sinter metal plate in the inlet of the plenum, which corresponds to a hard velocity inlet. The end of the combustion chamber is equipped with a perforated plate in all measurements in order to create a low reflective acoustic boundary condition. More details about the experimental set-up and measuring techniques can be found in [13] and [17].

NUMERICAL SET-UP AND BOUNDARY CONDITIONS

In Fig. 3, the geometry / computational domain of the axial swirl burner is presented. For URANS and LES, unstructured meshes with around 1.4 and 7.5 million cells were created, respectively. The plenum of the experimental test rig was not included in the computational domain in order to reduce computation requirements and to impose an excitation signal without resonance peaks in the power spectral distribution.

For LES, the Finite Volume based LES solver AVBP developed at CERFACS [16, 23] was used; and for the URANS, ANSYS CFX V12. The fully compressible multi-species Navier-Stokes equations are solved using a methane-air mixture with an equivalence ratio of 0.77 at atmospheric conditions for 30kW of power rating. The numerical set-up is detailed in Table 1.

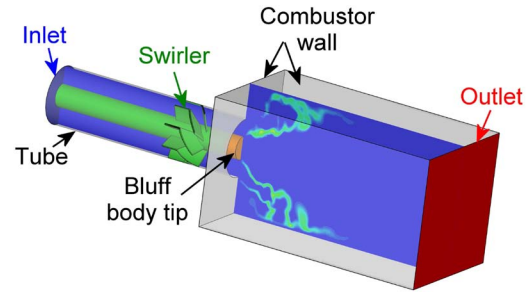

Figure 3. SCHEME OF THE NUMERICAL SET-UP OF THE BURNER.

Table 1. NUMERICAL SET-UP.

	URANS	LES
Turbulence/Sub-grid model	SST [24]	WALE [25]
Spatial/time Discretization	Second order	Second order
Time step [s]	5e-5	1.25e-7
Combustion model	TFC [22]	DTFM [21] (F=5)

The use of non-reflective boundary conditions (NRBC) is highly recommended to avoid the development of resonance modes, which can degenerate the identification process due to an ill-conditioned auto-correlation matrix [5]. For the URANS, partially reflecting boundary conditions based on the characteristics-based formulation of Poinsot and Lele [26] were used. For the LES, Kaess et al. [27] developed a modified version of the non-reflecting boundary conditions of Polifke et al. [28], which in turn are based on [26]. No inflow turbulence was introduced on the LES. Simulations were carried out considering non-adiabatic conditions at the combustor walls for correct flame stabilization [13, 16]. The non-adiabatic combustor walls and the bluff body tip are no-slip isothermal walls with a temperature of 600K, which is estimated from wall temperature measurements performed in another combustor at similar conditions [29]. The boundary conditions are indicated in Table 2 and shown in Fig. 3.

PRESENTATION AND VALIDATION OF CFD RESULTS

In Fig. 4, a snap shot of the instantaneous reaction rate from LES and the steady state reaction source term from RANS at the combustor middle cross plane is shown. Due to the Arrhenius formulation of the DTFM, heat loss effects on the reaction rate are captured, resulting in quenching of the reaction in the outer shear layer. For the RANS, strong reaction is present in the outer

Copyright © 2011 by ASME

Table 2. BOUNDARY CONDITIONS

B. Condition	Type	Details
Inlet	Non-reflec. velocity inlet	V=11.3 m/s
Outlet	Non-reflec. pressure outlet	P=101325 Pa
Combustor wall	Isothermal no slip wall	T=600 K
Tube/swirler	Adiabatic no slip wall	-
Bluff body tip	Isothermal no slip wall	T=600 K

shear layer. The TFC combustion model does not include effects of heat losses on the reaction source term. Similar behavior was observed using other RANS combustion models. A enhanced formulation including the combined effects of heat loss and strain will be presented in [30], but has not been evaluated in the present study.

In experiments, heat release is obtained using the line-of-sight integrated OH Chemiluminescence as indicator. To compare experiments with simulations, the averaged heat release from CFD was integrated over the depth of the combustion chamber, in order to determine the distribution in correspondence to the line-of-sight integrated view. The averaging interval for the LES was 87.5 ms. In Fig. 5, the normalized (with its maximum value) spatial distribution of OH chemiluminescence and heat release from experiments and simulations, respectively, are shown. Good agreement was found between LES and experiments due to the correct flame stabilization predicted in the simulations [13]. In Fig. 6, the axial heat release distributions from experiment and simulations are shown. The values are normalized taking into account that the area of the distribution from experiments and simulations should be the same, because the same amount of fuel is burnt in both cases. For the LES, good agreement was achieved, but with a slight difference in the position of the maximum heat release. The RANS underpredicts flame length due to the incorrect flame stabilization, presenting significant reaction in both shear layers. The intense reaction close to the burner exit in the RANS simulations is because the reaction source term of the TFC model is proportional to the gradient of the progress variable, which is large in the shear layers. The flame lengths (l_f), computed as the position of the maximum heat release, were 40.3, 45 and 25 mm, for the experiments, LES and URANS, respectively. Flow field measurements were not performed at this power rating, but a comparison for other power rating between LES and experiments is shown in [13]. Comparing the axial velocity from LES and RANS with reacting flow, the LES presents a shorter and wider inner recirculation zone than the RANS. Additionally, the inner recirculation zone in the LES extends slightly inside the burner.

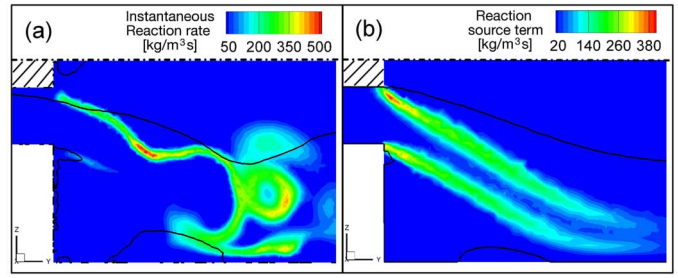

Figure 4. DISTRIBUTION OF REACTION RATE IN COMBUSTOR MIDDLE CROSS PLANE (SEE FIG. 3). LEFT: SNAP SHOT OF INSTANTANEOUS FROM LES. RIGHT: STEADY STATE SOURCE TERM FROM RANS. ZERO MEAN AXIAL VELOCITY ISOLINES IN BLACK.

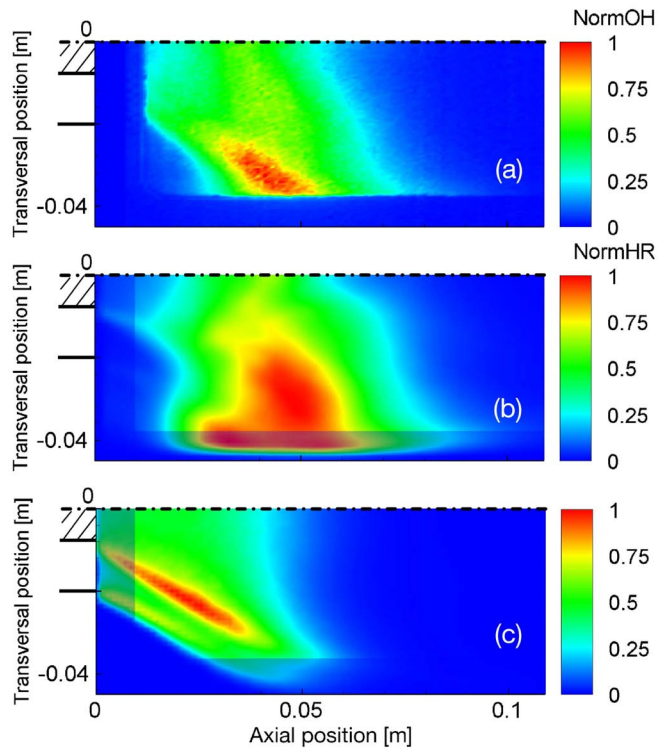

Figure 5. NORMALIZED SPATIAL DISTRIBUTION OF HEAT RELEASE: (a) OH* FROM EXPERIMENTS, (b) AVERAGED LES AND (c) RANS. LINE-OF-SIGHT INTEGRATED HEAT RELEASE. DUMP PLANE OF COMBUSTOR AT AXIAL POSITION=0m.

Comparison of Flame Transfer Functions

The simulations were excited at the inlet by perturbations on the characteristic ingoing wave with a broadband frequency-limited (1 kHz) discrete random binary signal [11] and an amplitude of 9.5% of the mean inlet velocity. The excitation amplitude was increased compared to the one applied in [13] (6.5%) to increase the signal-to-noise ratio, which improves the identification process. The flame response is still considered linear

Copyright © 2011 by ASME

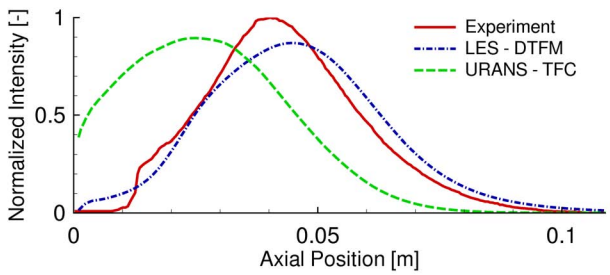

Figure 6. AREA NORMALIZED AXIAL HEAT RELEASE DISTRIBUTION.

for this amplitude [8]. The identification accuracy can be affected if the signals are influenced by strong levels of noise (e.g., from strong turbulence fluctuations) as shown in [13] and [19]. The simulation for all cases was run for 350 ms in real time (2.8 million and 7000 iterations for the LES and URANS, respectively). The acoustic velocity fluctuations were obtained 7 cm upstream of the burner exit. For the identification process, the first 25ms were not taken into account as they were considered as a transition period. The signals were then filtered to remove frequency content higher than 600Hz. In Fig. 7, the FTFs from experiments, LES/SI and URANS/SI are presented. All of them present amplitudes with a local maximum in gain above unity, followed by a decrease at higher frequencies. Good agreement was found between experiments and LES in amplitude and phase for frequencies lower than 200Hz. In LES, the resolved turbulent fluctuations result in a low signal-to-noise ratio for the higher frequencies, where the coherent flame response is weak as shown in [13]. The FTF identified with URANS presents similar characteristics as the FTFs from LES and experiment, but with a smaller maximum amplitude and with some modulations in the phase. The phase from URANS simulations is smaller than the one from experiments and LES, because the flame stabilizes in both shear layers, creating a shorter flame and reducing the time-lag responses of the flame to the different perturbations (mainly from mass flow and swirl number fluctuations [7, 9, 13, 17]). The phase error from URANS increases with frequency, increasing the discrepancies with respect to the experimental FTF. At higher frequencies, the URANS captured the "trend" of the experimental FTF somewhat better than LES. In URANS, signal-to-noise ratios are expected to be higher than in LES because turbulent fluctuations are not resolved. Nevertheless, the flame dynamics are better described using LES. There is a compromise between accuracy and computational time using URANS and LES. This might be reduced with the development of better combustion and turbulence models for URANS that can reproduce more accurately the flame characteristics (stabilization, length, etc.) and flow field. An evaluation using the two time-lag model from [17] has shown that the convective time lags from the mass flow fluctuations, defined by the ratio between the position of maximum heat release of the flame and a reference velocity representing the convective velocity of the perturbation along the shear layer, are 28.5 [13], 32.5 and 19ms for the FTF from experiments, LES and URANS, respectively. This agrees with the different flame lengths from experiments and simulations.

Confidence Analysis

The quantitative determination of measurement error for the FTF is complicated, because a long sequence of post-processing steps stands between the raw data and the final result. This is also true for CFD/SI based error estimates. Nevertheless, two methods were developed to analyze the statistics of the acquired data from simulations and experiments and determine associated standard deviations. For the simulations, a method based on bootstrapping [31] was used. The idea is to create artificial new data by randomly drawing elements from the original data set. Some elements will be chosen more than once. The procedure is repeated around 1000 times and statistical distributions of amplitude and phase are obtained. Standard deviations are computed from the distributions, indicating a measure of the deviation of the FTF identification by different levels of noise in the signal. In our case, this random process must be done to the correlation pairs obtained from Eq. (3) and (4), because they keep the correlation information between our original signals and responses. This procedure gives us a level of confidence that if the identification would have been repeated with another signal, the results would be between this range. For the experiments, the data was taken with a frequency of 10kHz for a total time of 40s for each single frequency. Then, multiple sequences of 15s from this data (e.g., the first interval from 0 to 15s, the next from 0.05 to 15.05 s, until 40 s) are created, and by a Fast Fourier Transform (FFT), statistical distributions of amplitude and phase are computed for each frequency. The standard deviation indicates possible deviations created by noise included in the acquired data. The deviation percentage as the standard deviation over the mean of the amplitude of the FTF is shown in Fig. 7. Deviations lower than 2% are mostly found in the data. The LES presents increased deviations for frequencies higher than 300Hz, indicating a higher influence of noise at that frequencies.

Stability Analysis

A final step after the identification of the FTFs is the stability analysis. Results of both LES and URANS show qualitative agreement with the experiments. But, how significant are quantitatively these discrepancies? To look at the impact of the discrepancies in the identified FTFs on predicting stability limits, a stability analysis was carried out with the network model tool "taX" [6] developed at TU Munich to evaluate and compare their eigenfrequencies and growth rates. The different elements are shown in Fig. 2 and their description is presented in Table 3.

Copyright © 2011 by ASME

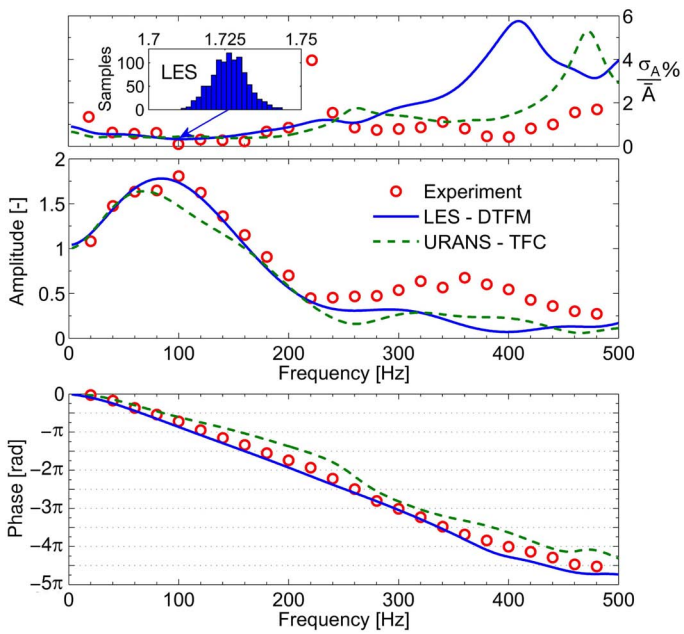

Figure 7. FLAME TRANSFER FUNCTION. TOP: CONFIDENCE ANALYSIS INCLUDING A HISTOGRAM OF AMPLITUDES FROM LES AT 100HZ FOR 1000 SEQUENCES

In experiments, an unstable eigenfrequency was found at 101.3Hz with a combustor length of 700 mm. There is uncertainty about the boundary conditions (reflection coefficients) of the experiments. For the stability analysis, the reflection coefficients measured by Alemela (in [32]) in a similar cross section combustor and perforated plate, but with another swirl burner, power rating (50kW) and equivalence ratio (0.735) were used, see Fig. 8

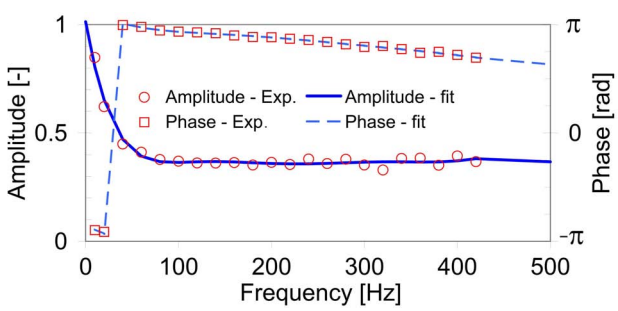

Figure 8. DOWNSTREAM REFLECTION COEFFICIENT USED IN NETWORK MODEL

One of the central aims of the paper is to evaluate the sensitivity of eigenfrequencies and cycle increments against slight differences in FTFs. For such comparative analysis, the length of the combustor on the network model (l_{comb}) was changed from 0.7 to 1 m in steps of 0.1 m keeping the same boundary conditions for all cases. After that, the eigenfrequencies and the growth rates were compared for the different lengths. A similar procedure was done experimentally and for network models by Kim et al. [8] to analyze the instability of the system and obtain eigenfrequencies. In Fig. 9, the eigenfrequencies obtained with the network model for the different combustor lengths are presented. 3 modes are observed : Mode (a) - produced by a Helmholtz resonance of the plenum and the connecting tube, Mode (b) - produced by the flame dynamics, and Mode (c) - corresponding to the 1/4 wave mode of the combustor, and decreasing with combustor length. The eigenfrequencies of modes (a) and (c) do not depend in a sensitive manner on the FTFs, as they are governed by the acoustics of the system.

Mode (b) is in the frequency range, where instabiliy was observed in experiment, and where the FTFs show their maximum amplitude. For this mode, the phase difference between the experiment and simulation is around $\pm\pi/8$ rad at 100 Hz. This is due to the differences in flame length, resulting in corresponding changes in eigenfrequencies. The trend of the eigenfrequencies is in agreement with the different flame lengths of the three cases. The flame length is an important parameter in determining self-excited eigenfrequencies [8]. Of course, more interesting in the stability analysis is to know if the eigenmode is stable or unstable. This is evaluated by the cycle increment (CI). As the unstable eigenfrequency from the experiment was found for mode (b), only the CIs for this zone are presented. The mode is strongly damped for (a), and marginally unstable modes for some lengths were observed in (c). In Fig. 10, the CIs for

Table 3. NETWORK MODEL.

Name	Details
Closed end	u'=0, R=1, T=293 K
Plenum	l=0.17 m, T=293 K
Area change 1	Compact element with losses [5], A_i= 0.031416 m^2, A_j= 0.001056 m^2
Tube 1, 2 and 3	l_1=0.11 m, l_2=0.025 m and l_3=0.045 m. T=293 K
Swirler	Swirler Transfer Matrix identified using LES/SI
Area change 2	Compact element with losses [5], A_i=0.001056 m^2 A_j= 0.0081 m^2
Combustor 1	l=l_f, T=293 K
Flame	Transfer Matrix model nTauPhi in [6]
Combustor 2	l=l_{comb} - l_f ,T=1930 K
Reflective end	Reflection coefficient from Fig. 8. T=1930 K

Copyright © 2011 by ASME

zone (b) with different combustor lengths are presented. The CIs using the FTF from experiments and LES are quite similar and are unstable for all evaluated combustor lengths. The CIs using the URANS FTF are much lower than the ones using the experimental FTF. The system becomes mainly unstable from L_{comb} higher than 1m. The good agreement between stability conditions using the FTFs from LES and experiments is because they present slight differences in the amplitude of the FTF. An amplitude in the FTF higher than 1 represents that the flame acts as an amplifier [10]. If the amplitude is increased, this effect will also increase. The amplitudes of the FTF from URANS are lower in the frequency range of the instability, resulting in lower cycle increments as shown in Fig. 10. This indicates the necessity of a correct identification of the amplitude of the FTF to predict growth rates, which was achieved only using LES.

CONCLUSIONS

URANS and LES of turbulent reacting flow were carried out in order to identify the flame transfer function (FTF) of a premixed swirl burner. Results for flame transfer functions and combustor stability were validated against experiment. The impact of inaccuracies in FTF prediction on frequencies and cycle increments of thermoacoustic eigenmodes was assessed with a low order model. Comparing the heat release distribution with experiment, LES presents good agreement, with only a slight difference in the position of the maximum heat release. URANS results obtained with the TFC combustion model predict a shorter flame, due to an unphysical flame stabilization pattern with intense reaction in the two shear layers between the annular jet of premixture, and the inner and outer recirculation zones, respectively.

For the LES-based FTF, good quantitative agreement with experiment was achieved, in particular for frequencies below 200 Hz. The FTFs from URANS present characteristics that are qualitatively similar to LES and experiment, but with reduced maximum amplitude and phase lag. The latter is related to the underpredicted flame length. Stability analysis of the test rig with the low-order taX model indicates that even small differences in predicted FTF may have a significant impact on growth rates. Stability behavior in agreement with experimental observation was obtained only with the LES-based FTF. This emphasizes the need for highly accurate turbulent combustion models when predicting flame dynamics and its impact on thermoacoustic combustion stability.

ACKNOWLEDGMENT

The authors gratefully acknowledge the financial support by the DAAD and the KW21-GV6 project, and to Stephan Föller for the implementation of the statistical evaluation tool for the FTF. We are indebted to CERFACS for making available the solver AVBP and to the Leibniz Rechenzentrum for providing access to HPC resources. Robert Leandro has supported the low-order modelling work with the taX package.

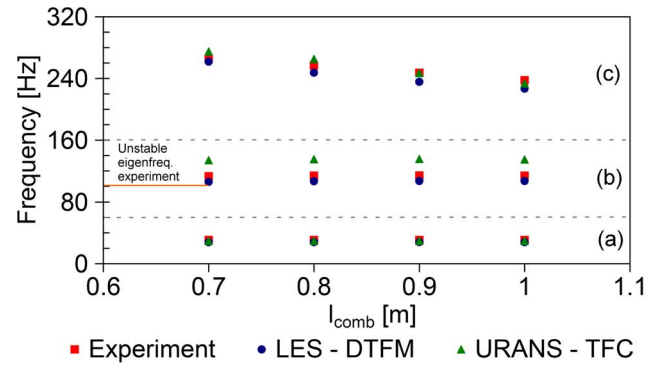

Figure 9. EIGENFREQUENCIES AT DIFFERENT COMBUSTOR LENGTHS IN NETWORK MODEL.

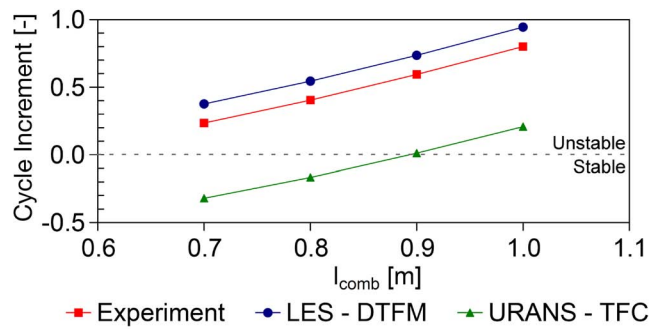

Figure 10. CYCLE INCREMENT IN MODE (b) FROM FIG. 9.

REFERENCES

[1] Keller, J., 1995. "Thermoacoustic Oscillations in Combustion Chambers of Gas Turbines". *AIAA Journal,* ***33***(12), pp. 2280–2287.

[2] Lieuwen, T., and Yang, V., 2005. *Combustion Instabilities in Gas Turbine Engines: Operational Experience, Fundamental Mechanisms and Modelling*. American Institute of Aeronautics and Astronautics, Reston, VA.

[3] Lawn, C. J., and Polifke, W., 2004. "A Model for the Thermo-acoustic Response of a Premixed Swirl burner: Part II: The Flame Response". *Combust. Sci. Technol.,* ***176***(8), pp. 1359–1390.

[4] Poinsot, T., and Veynante, D., 2005. *Theoretical and Numerical Combustion*, 2 ed. Edwards, R. T. Incorporated.

[5] Polifke, W., 2010. "Low-order Analysis Tools for Aero- and Thermo-Acoustic Instabilities". In *Advances in Aero-Acoustics and Thermo-Acoustics*, C. Schram, ed. Van Karman Inst for Fluid Dynamics., Brussels.

Copyright © 2011 by ASME

[6] Leandro, R., Huber, A., and Polifke, W., 2010. taX - a low-order modeling tool for thermo- and aero-acoustic instabilities. Tech. rep., TU München. www.td.mw.tum.de/tum-td/en/forschung/infrastruktur/scientific_comp.

[7] Palies, P., Durox, D., Schuller, T., and Candel, S., 2010. "The Combined Dynamics of Swirler and Turbulent Premixed Swirling Flames". *Combust. Flame,* ***157***, pp. 1698–1717.

[8] Kim, K., Lee, H., Lee, J., Quay, B., and Santavicca, D., 2009. "Flame Transfer Function Measurement and Instability Frequency Prediction Using a Thermoacoustic Model". No. GT2009-60026 in Proc. of ASME Turbo Expo 2009, Orlando, ASME.

[9] Hirsch, C., Fanaca, D., Reddy, P., Polifke, W., and Sattelmayer, T., 2005. "Influence of the Swirler Design on the Flame Transfer Function of Premixed Flames". No. GT2005-68195 in Proc. of ASME Turbo Expo 2005, Reno, ASME.

[10] Schuller, T., Durox, D., and Candel, S., 2003. "A Unified Model for the Prediction of Laminar Flame Transfer Functions: Comparisons between Conical and V-Flame Dynamics". *Combust. Flame,* ***134***, pp. 21–34.

[11] Huber, A., and Polifke, W., 2009. "Dynamics of Practical Premixed Flames, Part II: Identification and Interpretation of CFD Data". *International Journal of Spray and Combustion Dynamics,* ***1***(2), pp. 229–250.

[12] Polifke, W., Poncet, A., Paschereit, C. O., and Döbbeling, K., 2001. "Reconstruction of Acoustic Transfer Matrices by Instationary Computational Fluid Dynamics". *J. of Sound and Vibration,* ***245***(3), pp. 483–510.

[13] Tay Wo Chong, L., Komarek, T., Kaess, R., Föller, S., and Polifke, W., 2010. "Identification of Flame Transfer Functions from LES of a Premixed Swirl Burner". No. GT2010-22769 in Proc. of ASME Turbo Expo 2010, Glasgow, UK, ASME, p. 13.

[14] Polifke, W., 2010. "System Identification for Aero- and Thermo-Acoustic Applications". In *Advances in Aero-Acoustics and Thermo-Acoustics*, C. Schram, ed. Van Karman Inst for Fluid Dynamics., Brussels.

[15] Giauque, A., 2007. "Fonctions de Transfert de Flamme et Energies des Perturbations dans les Ecoulements Reactifs". PhD Thesis, Institut National Polytechnique, Toulouse.

[16] Schmitt, P., Poinsot, T., Schuermans, B., and Geigle, K. P., 2007. "Large-eddy Simulation and Experimental Study of Heat Transfer, Nitric Oxide Emissions and Combustion Instability in a Swirled Turbulent High-pressure Burner". *J. Fluid Mech.,* ***570***, pp. 17–46.

[17] Komarek, T., and Polifke, W., 2010. "Impact of Swirl Fluctuations on the Flame Response of a Perfectly Premixed Swirl Burner". *J. Eng. Gas Turbines Power,* ***132***, p. 061503.

[18] Kopitz, J., Bröcker, E., and Polifke, W., 2005. "Characteristics-based Filter for Identification of Planar Acoustic Waves in Numerical Simulation of Turbulent Compressible Flow". 12th Int. Congress on Sound and Vibration, Lisbon.

[19] Huber, A., 2009. "Impact of Fuel Supply Impedance and Fuel Staging on Gas Turbine Combustion Stability". PhD Thesis, Technische Universität München.

[20] Colin, O., Ducros, F., Veynante, D., and Poinsot, T., 2000. "A Thickened Flame Model for Large Eddy Simulations of Turbulent Premixed Combustion". *Phys. Fluids,* ***12***(7), pp. 1843–1863.

[21] Legier, J., Poinsot, T., and Veynante, D., 2000. "Large Eddy Simulation Model for Premixed and Non-premixed Turbulent Combustion". Proc. 2000 Summer Program, Center for Turbulence Research, Stanford, USA, pp. 157–168.

[22] Zimont, V., and Lipatnikov, A., 1995. "A Numerical Model of Premixed Turbulent Combustion of Gases". *Chem. Phys. Reports,* ***14***(7), pp. 993–1025.

[23] CERFACS. http://www.cerfacs.fr/4-26334-The-AVBP-code.php.

[24] Menter, F., Kuntz, M., and Langtry, R., 2003. "Ten Years of Industrial Experience with the SST Turbulence Model". In Turbulence, Heat and Mass Transfer 4, K. Hanjalic, Y. Nagano, and M. Tummers, eds., Begell House, Inc., pp. 625–632.

[25] Nicoud, F., and Ducros, F., 1999. "Subgrid-scale Stress Modeling Based on the Square of the Velocity Gradient Tensor". *Flow Turb. Combust.,* ***62***, pp. 183–200.

[26] Poinsot, T., and Lele, S., 1992. "Boundary Conditions for Direct Simulation of Compressible Viscous Flows". *J. Comput. Phys.,* ***101***, pp. 104–129.

[27] Kaess, R., Huber, A., and Polifke, W., 2008. "Time-domain Impedance Boundary Condition for Compressible Turbulent Flows". No. AIAA 2008-2921 in 14th AIAA/CEAS Aeroacoustics Conference, Vancouver, AIAA.

[28] Polifke, W., Wall, C., and Moin, P., 2006. "Partially Reflecting and Non-reflecting Boundary Conditions for Simulation of Compressible Viscous Flow". *J. Comput. Phys.,* ***213***, pp. 437–449.

[29] Fanaca, D. (Private communication).

[30] Tay Wo Chong, L., Komarek, T., Zellhuber, M., and Polifke, W., 2011. "Influence of Strain and Heat Loss on Flame Stabilization in a Non-Adiabatic Combustor". *To be submitted in Flow Turb. Combust.*

[31] Efron, B., and Tibshirani, R., 1993. *An Introduction to the Bootstrap*. Chapman & Hall.

[32] Wanke, E., 2010. "FE-Verfahren zur Analyse der Thermoakustischen Stabilität nichtisentroper Strömungen". PhD Thesis, Technische Universität München.

Copyright © 2011 by ASME